Algebraic cubature on polygonal elements with a circular edge

E. Artioli[1], A. Sommariva[2] and M. Vianello[2]

October 14, 2019

Abstract

We ccompute low-cardinality algebraic cubature formulas on convex or concave polygonal elements with a circular edge, by subdivision into circular quadrangles, blending formulas via subperiodic trigonometric Gaussian quadrature and final compression via Caratheodory-Tchakaloff subsampling of discrete measures. We also discuss applications to the VEM (Virtual Element Method) in computational mechanics problems.

2010 AMS subject classification: 65D32, 65N30.

Keywords: algebraic cubature formulas, curved polygonal elements, cubature compression, Caratheodory-Tchakaloff subsampling, VEM (Virtual Element Method).

1 Introduction

The problem of efficient numerical integration over polygons has been object of great interest during the last fifteen years, mainly due to the developement and expansion of polygonal/polyhedral finite element models and methods; cf., with no pretence of exhaustivity, [2, 23, 25, 28, 29, 30, 37, 41, 42] with the references therein. On the other hand, the case of polygons with possible curved edges has also emerged in recent years, for example in connection with the VEM (Virtual Element Method), cf., e.g., [13, 14, 15].

In this paper, we consider a particular situation of interest in computational mechanics, namely the construction of algebraic cubature formulas, i.e. exact formulas on bivariate polynomials up to a given total degree, with low cardinality on polygonal elements with a circular edge. Convex as well as concave curved polygonal elements may appear by polygonal discretization, the concave ones typically in the presence of circular holes, and both kinds for example with a fibre-reinforced composite material; see Figures 1 and 4, and Figures 2 and 6.

We postpone to section 3 some introductive notions and technical considerations about the VEM. We only sketch here the computational approach for the construction of low-cardinality cubature formulas on polygonal elements with

[1]Department of Civil Engineering and Computer Science, University of Rome Tor Vergata, Italy
corresponding author: artioli@ing.uniroma2.it
[2]Department of Mathematics, University of Padova, Italy

a circular edge, which is essentially a discrete moment-matching technique, followed by a suitable compression stage.

The first step, described in subsections 2.1 and 2.2, consists of the element subdivision into "circular quadrangles" (possibly degenerating into asymmetric circular sectors), followed by the computation of product-like Gaussian quadrature on each quadrangle via arc blending and Gaussian quadrature on circular arcs (subperiodic trigonometric Gaussian quadrature, cf. [21, 22, 45]). Then, a final algebraic cubature formula for the curved element is immediately obtained by finite union, collecting together all the nodes and respective positive weights.

The second key step, discussed in subsection 2.3, is the compression of the overall formula on the element into a low-cardinality one, still with positive weights and keeping the polynomial exactness degree, by the Caratheodory-Tchakaloff subsampling methods for discrete measures discussed in [31, 39]. Numerical examples concerning applications to the VEM implementation in the framework of computational mechanics are discussed in detail in section 3.

We stress that, differently from other cubature approaches available in the literature (cf., e.g., [13, 38]), with the present specific element geometry we are able to provide low-cardinality cubature formulas that have in any case *internal* nodes, *positive* weights and guaranteed *polynomial exactness*.

2 Cubature construction

We shall consider an integration domain, say Ω with vertices $P_1, \ldots, P_\ell$, $\ell \geq 2$ (counterclockwise ordered), obtained from a *convex polygon*, say $\mathcal{P}$ with the same vertices, where the straight edge joining P_ℓ and P_1 is substituted by an arc $\widehat{P_\ell P_1}$ of a circle with center C and radius r (with no other intersection with the straight edges). Domains of this form are for example obtained by intersection or set difference of convex polygons with an overlapping disk, when the boundary circle intersects the polygon boundary at only two points. This is a typical situation with suitable polygonal meshes in the presence of holes, as we shall see in the application to the VEM.

When $\ell = 2$, the domain turns out to be a circular segment (one of the two portions of a disk cut by a straight line), when $\ell = 3$ is a *generalized* circular sector, while when $\ell = 4$ is more generally a *circular quadrangle*. Our aim is to describe Ω when $\ell \geq 4$ as a partition into circular quadrangles, possibly degenerating in generalized circular sectors or circular segments, and at most two convex polygons.

2.1 Domain subdivision

The simplest case is that of a convex edge $\widehat{P_\ell P_1}$ (i.e. the curved edge is outside the convex polygon $\mathcal{P}$), since the domain is simply the nonoverlapping union of $\mathcal{P}$ with a circular segment, say $\mathcal{S}$, see e.g. Figure 1. Observe that in general the domain could even be globally nonconvex.

The case of a concave edge (i.e. $\widehat{P_\ell P_1}$ is inside $\mathcal{P}$) turns out to be more complicated. Let (r_k, θ_k) be the polar coordinates (with respect to the circle center C) of the points P_k, for $k = 1, \ldots, \ell$, where $r_1 = r_\ell = r$ and $[\theta_1, \theta_\ell] \subset [0, 2\pi)$. It is not restrictive to assume $\theta_1 < \theta_\ell$ otherwise one simply rotates the

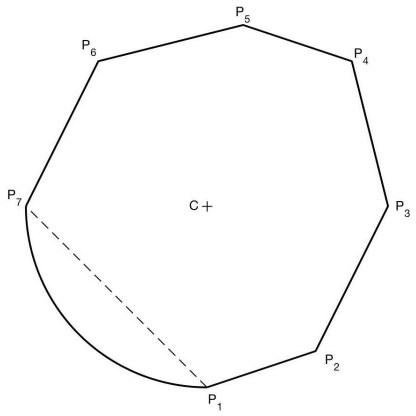

Figure 1: Example of domain Ω with a convex edge and its partitioning ($\ell = 7$).

domain so to satisfy this requirement. Observe that such a domain is always concave by construction.

We subdivide the vertices as follows:

- (i) $\{P_1, \ldots, P_{\ell_1}\}$ are consecutive vertices, whose polar angles are not in the open interval (θ_1, θ_ℓ);
- (ii) $\{P_{\ell_1+1}, \ldots, P_{\ell_2-1}\}$ are consecutive vertices of the polygon $\mathcal{P}$, whose polar angles are in (θ_1, θ_ℓ);
- (iii) $\{P_{\ell_2}, \ldots, P_\ell\}$ are consecutive vertices of the polygon $\mathcal{P}$, whose polar angle are again not in (θ_1, θ_ℓ), with $\ell_1 < \ell_2$.

This partitioning of the vertices can be easily understood in Figure 2.

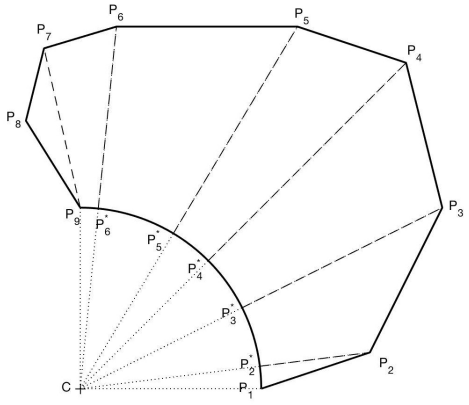

Figure 2: Example of domain Ω with concave edge and its partitioning ($\ell_1 = 1$, $\ell_2 = 7$, $\ell = 9$). In particular the only polygon of this partition is the triangle with vertices P_7, P_8, P_9.

We observe that there can be many particular cases, for instance the sets (i) or (iii) may reduce to a singleton, or the set of vertices (ii) may be empty. In

spite of this, the partition into (at most two) polygons and circular quadrangles, possibly degenerating in generalized circular sectors, is always possible.

Indeed, consider first the set of vertices (ii). If this is not empty, define P_k^*, $k = \ell_1 + 1, \ldots, \ell_2 - 1$, as the intersection point between the circular arc and the straight line passing between C and P_k. Alternatively, one can think of P_k^* as the point on the circular arc with the same polar angle θ_k of P_k (with respect to the circle center C). As a first step, one defines the circular quadrangles $\mathcal{Q}_k$, $k = \ell_1 + 1, \ldots, \ell_2 - 2$, whose boundary is defined by the segments $\overline{P_k^* P_k}$, $\overline{P_k P_{k+1}}$, $\overline{P_{k+1} P_{k+1}^*}$, and the subarc $\widehat{P_{k+1}^* P_k^*}$.

As further step one considers the circular quadrangles

- $\mathcal{Q}_{\ell_1}$ (possibly reducing to a circular sector or even to a segment), whose boundary is defined by the segments $\overline{P_1 P_{\ell_1}}$, $\overline{P_{\ell_1} P_{\ell_1+1}}$, $\overline{P_{\ell_1+1} P_{\ell_1+1}^*}$, and the subarc $\widehat{P_{\ell_1+1}^* P_1}$;
- $\mathcal{Q}_{\ell_2}$ (again possibly reducing to a circular sector or even to a segment), whose boundary is defined by the segments $\overline{P_{\ell_2-1}^* P_{\ell_2-1}}$, $\overline{P_{\ell_2-1} P_{\ell_2}}$, $\overline{P_{\ell_2} P_\ell}$, and the subarc $\widehat{P_\ell P_{\ell_2-1}^*}$.

We finally observe that the (closure of the) set $\Omega \setminus \bigcup_{k=\ell_1}^{\ell_2} \mathcal{Q}_k$ consists of (at most) two convex polygons.

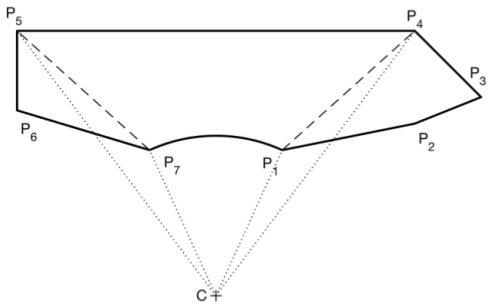

Figure 3: Example of domain Ω (concave case) where the set of vertices (ii) is empty, and its partitioning. Here, $\ell_1 = 4$, $\ell_2 = 5$, $\ell = 7$.

Alternatively, suppose that the set of vertices (ii) is empty; see Figure 3. In this case $\ell_2 = \ell_1 + 1$ and we simply define $\mathcal{Q}_{\ell_1} = \mathcal{Q}_{\ell_2 - 1}$ the circular quadrangle (possibly reducing to a generalized circular sector) whose boundary is defined by the segments $\overline{P_1 P_{\ell_1}}$, $\overline{P_{\ell_1} P_{\ell_1+1}}$, $\overline{P_{\ell_1+1} P_\ell}$, and the entire arc $\widehat{P_\ell P_1}$. Again, the (closure of) the set $\Omega \setminus \mathcal{Q}_{\ell_1}$ consists of (at most) two convex polygons.

Remark 1 *We note that, though our initial assumption is that the polygonal domain $\mathcal{P}$ is convex (as for example the elements generated via Voronoi tessellations), the case of a nonconvex $\mathcal{P}$ could be treated by preliminary splitting into nonoverlapping convex polygons; cf., e.g., the simple algorithm in [26].*

2.2 Algebraic cubature by arc blending

In the previous section we have shown that in the case of a convex circular edge, the integration domain Ω can be partitioned into into a convex polygon $\mathcal{P}$ and circular segment $\mathcal{S}$. In the more difficult case of a concave circular edge, the domain can be partitioned into a certain number of circular quadrangles, say $\{\mathcal{Q}_k\}$ (possibly generalized circular sectors) and (at most) two convex polygons, say $\mathcal{P}_1$, $\mathcal{P}_2$.

Thus, if we intend to obtain a cubature rule with algebraic degree of exactness $ADE = n$ on Ω, i.e.

$$\iint_{\Omega} p(x,y)\,dxdy = \sum_{i=1}^{M_n} w_i\, p(x_i,y_i)\ , \quad \forall p \in \mathbb{P}_n^2\ , \tag{1}$$

where $\mathbb{P}_n^2$ denotes the space of bivariate polynomials of total degree not exceeding n, by the additivity of integrals, it is sufficient to find formulas with the same property on polygons and circular quadrangles. Observe that generalized circular sectors are a special degenerate case of circular quadrangles, where the edge opposite to the curved one collapses into a point. Similarly, circular segments are special circular quadrangles where the opposite straight edges collapse into points.

In particular, if we are able to determine formulas with Positive weights and Interior nodes for both polygons and circular quadrangles, then one with the same features is available on the whole Ω collecting together nodes and weights of the partition pieces; we shall adopt the usual acronym PI for such formulas.

Concerning polygons, though a number of cubature methods are available in the literature (we have already given a partial list in the Introduction), we have followed the approach implemented by the codes in [36]. Since the relevant polygons are convex, they can be easily partitioned into a minimal number of triangles (two less than the number of edges), simply by taking triples of consecutive vertices. Then, it is sufficient to compute a PI cubature formula with $ADE = n$ in each triangle, taking a formula of this type for the simplex and using barycentric coordinates.

Well-known examples are Stroud's formulas whose cardinality is $(n+1)^2/4$ for odd n, but if available, one can use formulas attaining Möller's lower bound, namely $\nu_n = \dim\left(\mathbb{P}^2_{\lceil n/2\rceil}\right)$ (the so called *minimal formulas*). Minimal formulas on the simplex are known for example for $n = 1, 2, 3, 4, 5, 7$ and have respectively $1, 3, 4, 6, 7, 12$ nodes; cf., e.g., [19, 20] with the references therein. Alternatively, one could resort to several *near-minimal* formulas for the simplex obtained in the literature, whose cardinality is close to the lower bound; cf. [36] for a collection of minimal and near-minimal formulas up to degree 50.

Turning to circular quadrangles, a PI cubature formula with $ADE = n$ can be obtained adapting some arguments in [21], that rely on the basic concepts of *subperiodic trigonometric Gaussian quadrature* and circular *arc blending*. In the following, we shall denote by $\mathbb{P}_n$, $\mathbb{T}_n$ the univariate algebraic and trigonometric polynomials of degree not exceeding n, respectively.

Indeed, the basic observation is that a circular quadrangle $\mathcal{Q}$ can be written as a bilinear algebraic-trigonometric transformation of a rectangle, namely

$$\mathcal{Q} = \{(x,y) = \sigma(t,\theta) = tP(\theta) + (1-t)Q(\theta)\,,\ (t,\theta) \in [0,1]\times[\alpha,\beta]\}\ , \tag{2}$$

where in general $P(\theta)$ and $Q(\theta)$ are parametric curves with trigonometric components of degree 1, namely

$$P(\theta) = A_1 \cos(\theta) + B_1 \sin(\theta) + C_1 \ , \quad Q(\theta) = A_2 \cos(\theta) + B_2 \sin(\theta) + C_2 \ , \quad (3)$$

with $\theta \in [\alpha, \beta]$, $\beta - \alpha \leq \pi$, and $A_i, B_i, C_i \in \mathbb{R}^2$, $i = 1, 2$. We can call this transformation a "linear blending of subperiodic arcs", since the angles belong to a subinterval of the period. Several sections of a disk and other domains related to circular (or even elliptical) arcs can be obtained by a transformation of this kind, cf. [21, 22].

In the present context, let us call $V_i = (\xi_i, \eta_i)$, $i = 1, 2, 3, 4$ the consecutive vertices of the circular quadrangle (counterclockwise ordered), where $\widehat{V_1 V_4}$ is a circular arc of center $C = (x_0, y_0)$ and radius r (the other edges being straight segments), and let α, β be respectively the polar angles of V_1 and V_4 (with respect to C). Then, assuming $\beta - \alpha \leq \pi$ and setting $s = \sin(\frac{\beta-\alpha}{2})$ and $\phi = (\beta + \alpha)/2$, it is easily seen that a circular quadrangle is obtained by the transformation (2)-(3) with

$$A_1 = (r, 0) \ , \ B_1 = (0, r) \ , \ C_1 = C = (x_0, y_0) \ ,$$

$$A_2 = -\frac{\sin(\phi)}{2s} (V_3 - V_2) \ , \ B_2 = \frac{\cos(\phi)}{2s} (V_3 - V_2) \ , \ C_2 = \frac{1}{2} (V_3 + V_2) \ . \quad (4)$$

The first row of the formula above corresponds to the polar representation of the circular arc $\widehat{V_1 V_4}$, and the second row to a bijective trigonometric representation of the segment $\overline{V_2 V_3}$ via the same interval $[\alpha, \beta]$, as $(V_3 + V_2)/2 + \tau(V_3 - V_2)/2$, $\tau \in [-1, 1]$, with $\tau = \sin(\theta - \phi)/s = [\sin(\theta)\cos(\phi) - \cos(\theta)\sin(\phi)]/s$, $\theta \in [\alpha, \beta]$.

Now, as observed in [21], the transformation σ is injective whenever the curves parametrized by $P(\theta)$ and $Q(\theta)$, as well as any two segments $tP(\theta_1) + (1-t)Q(\theta_1)$, $tP(\theta_2) + (1-t)Q(\theta_2)$, $\theta_1, \theta_2 \in [\alpha, \beta]$, can mutually intersect only at an endpoint. Notice that this property holds for the circular quadrangles relevant to the present paper (cf. Figures 2-3), due to the geometric structure of the curved polygonal element Ω. Then the Jacobian $\det(J\sigma)$ has *constant sign* in the interior of $\mathcal{Q}$ and we can write for any $p \in \mathbb{P}_n^2$

$$\iint_{\mathcal{Q}} p(x, y)\, dxdy = \iint_{[0,1]\times[\alpha,\beta]} p(\sigma(t, \theta)) \, [\pm \det(J\sigma(t, \theta))] \, dtd\theta \ , \quad (5)$$

depending on the Jacobian sign, where

$$(p \circ \sigma) \, [\pm \det(J\sigma)] \in \mathbb{P}_{n+1} \otimes \mathbb{T}_{n+2} \ , \quad (6)$$

since $(p \circ \sigma) \in \mathbb{P}_n \otimes \mathbb{T}_n$ and $\det(J\sigma) \in \mathbb{P}_1 \otimes \mathbb{T}_2$.

Such a tensorial structure suggests to use a product quadrature, via algebraic Gaussian quadrature, provided that a good trigonometric quadrature formula is also available on subintervals of the period. This is indeed the case, by the following proposition on *subperiodic trigonometric Gaussian quadrature*, proved in [22] and used for example in [21].

Proposition 1 *Let $\{(\xi_j, \lambda_j)\}$, $1 \leq j \leq k+1$, be the nodes and positive weights of the algebraic Gaussian quadrature formula for the weight function*

$$w(x) = \frac{2\sin(\omega/2)}{\sqrt{1 - x^2 \sin^2(\omega/2)}} \ , \quad x \in (-1, 1) \ , \quad \omega \in (0, \pi] \ . \quad (7)$$

Then for $0 < \beta - \alpha \leq 2\pi$ *the following trigonometric Gaussian quadrature formula holds*

$$\int_{\alpha}^{\beta} f(\theta)\, d\theta = \sum_{j=1}^{k+1} \lambda_j\, f(\theta_j)\ , \quad \forall f \in \mathbb{T}_k\ , \tag{8}$$

where setting $\omega = (\beta - \alpha)/2$ *and* $\phi = (\beta + \alpha)/2$

$$\theta_j = \phi + 2\arcsin(\xi_j \sin(\omega/2))\ , \quad 1 \leq j \leq k+1\ . \tag{9}$$

We can now state the following proposition on the construction of a product Gaussian-like formula on circular quadrangles, whose proof is an easy consequence of Proposition 1 and (5)-(6), cf. [21] for the general blending case.

Proposition 2 *Let* $\mathcal{Q}$ *be a circular quadrangle of the form (2)-(4), where the transformation* σ *is injective. Then*

$$\iint_{\mathcal{Q}} p(x,y)\, dxdy = \sum_{j=1}^{n+2} \sum_{i=1}^{\lceil \frac{n+1}{2} \rceil} W_{ij}\, p(x_{ij}, y_{ij})\ , \quad \forall p \in \mathbb{P}_n^2\ , \tag{10}$$

where

$$(x_{ij}, y_{ij}) = \sigma(t_i^{GL}, \theta_j)\ , \quad 0 < W_{ij} = |det(J\sigma(t_i^{GL}, \theta_j))|\, w_i^{GL}\, \lambda_j\ , \tag{11}$$

$\{(\theta_j, \lambda_j)\}$ *being the angular nodes and weights of the trigonometric Gaussian formula of degree of exactness* $n+2$ *on* $[\alpha, \beta]$ *and* $\{(t_i^{GL}, w_i^{GL})\}$ *the nodes and weights of the Gauss-Legendre formula of degree of exactness* $n+1$ *on* $[0,1]$.

We have implemented the cubature formula (10)-(11) by the Matlab functions `trigauss` and `gqellblend` (trigonometric Gaussian quadrature and cubature via arc blending, respectively), that are available at [45]. Observe that the cardinality of such a formula is $(n+2)\lceil \frac{n+1}{2} \rceil = n^2/2 + \mathcal{O}(n)$.

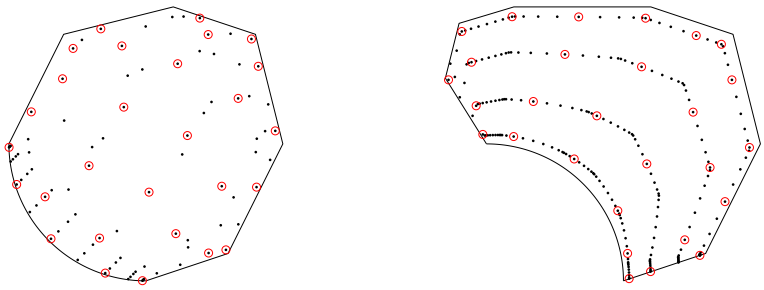

Figure 4: Convex and concave edge polygonal elements of Figures 1-2 with basic cubature nodes by splitting and arc blending (91 and 223 small dots, respectively), and compressed Caratheodory-Tchakaloff nodes (28 small circles), for $ADE = 6$.

2.3 Caratheodory-Tchakaloff cubature compression

In this subsection we show how a PI cubature formula with $ADE = n$ and a cardinality greater than

$$N = N_n = \dim\left(\mathbb{P}_n^2\right) = \binom{n+2}{2} = \frac{(n+1)(n+2)}{2} \tag{12}$$

can be compressed into a formula with the same properties, whose nodes are a re-weighted subset of the original ones with cardinality not exceeding N. We focus here on the bivariate discrete case, recalling however that this result is valid in full generality for any discrete or continuous measure in any dimension, by the celebrated Tchakaloff's theorem; cf., e.g., [33]. We give below the main lines of the construction, following [31] where the general case of discrete measures in any dimension is treated.

Consider an algebraic cubature formula like (1) on a domain $\Omega \subset \mathbb{R}^2$, with $M = M_n > N$, where $X = \{(x_i, y_i)\}$ is the set of M_n nodes and $w = \{w_i\}$ the array of positive weights. Let $\{p_1, \ldots, p_N\}$ be a basis of $\mathbb{P}_n^2$ and define the corresponding Vandermonde-like matrix

$$V = V_n(X) = [v_{ij}] = [p_j(x_i, y_i)] \in \mathbb{R}^{M \times N} \ . \tag{13}$$

Then, looking for a PI cubature formula whose support is a subset of X, is equivalent to finding a *sparse* solution with less than M nonzeros, of the underdetermined *moment matching system* with nonnegativity constraints

$$V^t u = b = V^t w \ , \quad u \geq 0 \ . \tag{14}$$

Now, by the celebrated Caratheodory's theorem on finite-dimensional conic combinations [18], applied to the columns of V^t, we know that such a sparse nonnegative solution exists (not necessarily unique) and that the number of nonzeros does not exceed N. If u is any such solution, calling $\{i_k\}$, $1 \leq k \leq m \leq N < M$, the indexes such that $u_{i_k} \neq 0$, we have

$$\iint_\Omega p(x, y)\, dxdy = \sum_{i=1}^{M} w_i\, p(x_i, y_i) = \sum_{k=1}^{m} u_{i_k}\, p(x_{i_k}, y_{i_k}) \ , \quad \forall p \in \mathbb{P}_n^2 \ . \tag{15}$$

In view of the theoretical tools, following [31] we may call the resulting cubature formula a *Caratheodory-Tchakaloff* (CATCH) compressed cubature formula.

The computation of Caratheodory-Tchakaloff cubature formulas (or cubature measures under a more probabilistic point of view) has been object of some attention in the recent numerical literature; cf., e.g., [31, 39, 44] with the references therein. Two main approaches have been pursued. Notice that the problem does not fall readily in the class solvable by the most usual compressed sensing techniques, such as the well-known *Basis Pursuit* [24], which work on ℓ^1-norm minimization, because by construction here the ℓ^1-norm of the weights is constant, namely $\|w\|_1 = \|\{u_{i_k}\}\|_1 = area(\Omega)$.

A first one is a Linear Programming approach, consisting in solving via the simplex method

$$\begin{cases} \min c^t u \\ V^t u = b \ , \quad u \geq 0 \end{cases} \tag{16}$$

where the constraints identify a polytope in $\mathbb{R}^M$ (the feasible region, which is nonempty since $b = V^t w$) and the vector c is chosen to be linearly independent from the rows of V^t, so that the objective functional is not constant on the polytope. As known the simplex method computes a vertex of the poytope, that has at least $M - N$ vanishing components.

A second approach is based on Quadratic Programming, requiring the solution of the NonNegative Least Squares (NNLS) problem

$$\text{compute } u^* : \|V^t u^* - b\|_2 = \min_{u \geq 0} \|V^t u - b\|_2 \,, \tag{17}$$

where u^* can be determined by the well-known *Lawson-Hanson* active set optimization method [27], that computes a sparse solution to (17). Several versions of the Lawson-Hanson method are available in Matlab. One is the built-in function `lsqnonneg`, while an open-source version is downloadable from the package NNLSlab [35]. Other versions require the use of MEX files and will not be used here. Our numerical experience has shown that for moderate degrees (say $n \leq 20$), which are the target of the applications in the present paper, the residual $\varepsilon = \|V^t u^* - b\|_2$ is always around machine precision and the NNLS approach turns out to be more efficient than the LP approach.

We have applied Caratheodory-Tchakaloff compression to the basic cubature formula on polygonal elements with a circular edge, obtained via splitting of the element into circular quadrangles and polygons, as discussed in the previous subsections. The same compression technique can also be applied to standard polygonal elements with straight edges appearing in FEM/VEM applications (see Figure 5 and 7 below), cf. [10]. As polynomial basis, in order to avoid the extreme ill-conditioning of Vandermonde matrices arising for example with the standard monomial basis, we have chosen the total-degree product Chebyshev basis of the smallest Cartesian rectangle containing the element.

To give an idea of the performance of the method with degrees of exactness suitable to FEM/VEM applications, we present the following table, where we have collected the cputimes for the construction of the basic formula and of the compression phase on the convex and concave curved polygonal elements of Figure 4, for $ADE = n = 2, 4, 6$. The numerical tests tests have been performed in Matlab R2017b on a 2.7 GHz Intel Core i5 with 16GB 1867MHz DDR3 memory.

The results are encouraging, in view of large-scale applications. For example in the concave element test case (9 edges) at degree $n = 6$, the basic formula with 223 nodes and its compression into 28 nodes are constructed with a total cputime in the order of milliseconds.

3 VEM benchmarks (computational mechanics)

The present section is devoted to the application of the proposed cubature formula for curved polygons to the solution of two benchmark problems stemming from computational mechanics with the Virtual Element Method (VEM). The VEM has been recently introduced [14, 15] as a generalization of the Finite Element Method for the approximation of partial differential equations. It is a Galerkin method which presents numerous interesting features, many of which are not feasible in a standard FEM context. In particular, the VEM method

Table 1: Average cputimes (seconds) for the computation of the basic cubature formula and of the Caratheodory-Tchakaloff (CATCH) compressed cubature formula on the polygonal elements of Figure 4.

degree n	2	4	6
CONVEX edge			
cputime BASIC	1.2e-3 s	1.2e-3 s	1.2e-3 s
cputime CATCH	8.0e-4 s	9.0e-4 s	2.0e-3 s
cputime total	2.1e-3 s	2.1e-3 s	3.2e-3 s
CONCAVE edge			
cputime BASIC	4.6e-4 s	4.7e-4 s	4.8e-4 s
cputime CATCH	4.5e-4 s	1.6e-3 s	2.5e-3 s
cputime total	9.1e-4 s	2.1e-3 s	3.0e-3 s

can deal with complex domain geometries via general polytopal meshes, which allow for hanging nodes, efficient local mesh refinement, adaptivity, and, as it will be made clear in the following, curvilinear polygons. Although approximation spaces are not known explicitly for a VEM method, they can be built so to fulfill internal constraints, high continuity requirements and, in general, as the solution of particular PDEs systems. All in all, the VEM can represent an interesting alternative from the standard FEM in many mathematical and engineering applications.

In regard to linear elasticity problems, where VEM has been already applied in numerous situations [11, 12, 17, 25], in the present investigation, attention will be given to a newly proposed version of the method, which is capable of using general polygons with curved edges [13]. The interest towards this particular capability resides in the fact that problems posed on curved physical domains can be approximated annihilating the geometric rectification error on curvilinear domain boundary portions, while the same does not hold true with standard straight-edge finite element approximations. Moreover, curved virtual elements are shown to have optimal rate of convergence and higher accuracy with respect to straight-edge VEM.

Motivated by the above mentioned facts, and to prove applicability of our cubature formula in structural analysis simulations, we present a selected numerical campaign with curved virtual elements adopting the proposed cubature scheme. As previously stated, a key feature of this formula is that it grants all interior nodes and all positive weights, regardless of curved edge convexity. The latter is a remarkable feature for solid and structural mechanics applications, especially when dealing with material nonlinearity [5], as, typically, cubature node locations are connected to the evaluation of constitutive properties for the material body under investigation and hence need be interior to it for their evaluation to make sense.

In the following two sections, details on problem formulation, VEM discretization and result post-processing for the two investigated cases are omitted for brevity, as they can be found in [43, 4], and in [6, 3], respectively.

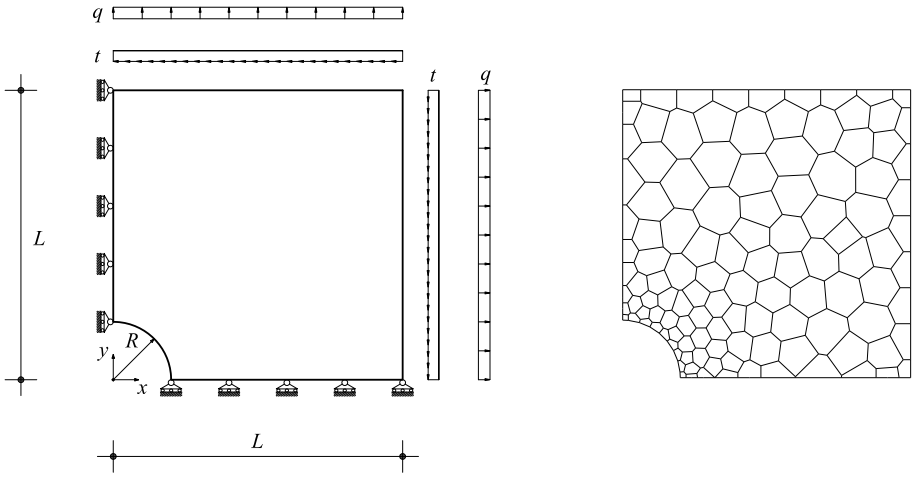

Figure 5: Infinite plate with hole. Left: geometry, boundary conditions, loading for the computational domain. Right: representative Voronoi tessellation for VEM analysis.

3.1 Infinite plate with circular hole

The first benchmark is an infinite plate with a central circular hole under uniform unit traction along horizontal x direction. The exact solution of this problem, in polar coordinates, can be found in [43].

Fig. 5 shows the finite computational domain exploiting double symmetry, in which a square domain with a circular hole, with radius $R = 1$, is considered assuming a side-to-radius ratio of 5. Plane stress conditions are invoked. Material properties are chosen as: Young's modulus $E = 10^5$ units and Poisson's ratio $\nu = 0.3$. Tractions corresponding to the analytical solution are applied on the right and top edges, while Dirichlet homogeneous symmetry boundary conditions are applied on the left and bottom edges [43].

Resorting to a Voronoi polygonal tessellation, as depicted in Fig. 5, an accuracy and convergence rate study with quadratic VEM is carried out. Starting from an initial ad-hoc mesh with appropriate refined elements around the circular hole and comprising polygons having each a curved circular edge, we plot the L^2 relative error norm for the Cauchy stress, considering uniform mesh refinements. As it can be observed in Fig. 6, the VEM structural analysis adopting curved polygons in conjunction with the proposed cubature formula shows optimal convergence rate and excellent accuracy levels. A further remark in favor of the proposed approach is that the convergence rate $O(h_E^2)$, as reported in Figure 8, is correctly obtained due to the fact that the geometric parametrization of the circular boundary of the fibre is *exactly* taken into account by the curvilinear VEM formulation, while it is known (see [13, 7] for instance) that

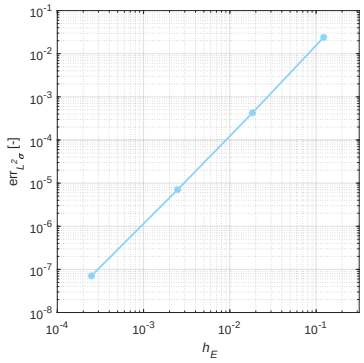

Figure 6: Infinite plate with hole. L^2 error norm for the Cauchy stress *vs* mesh size h_E for $k = 2$ VEM approximation.

only a suboptimal rate would be expected with a standard (i.e. straight-edge) VEM-like (or FEM-like) approach with piecewise linear geometry parametrization of the curve; the same issue would hold for $k = 2$, yielding a suboptimal $O(h_E^{3/2})$ error behavior in the same norm.

3.2 Fibre-reinforced composite material (homogeneization)

The second benchmark is related to a classical problem from constitutive modeling of advanced materials, namely computational homogenization for fibre-reinforced composite materials. In the realm of asymptotic homogenization theory [16, 34], the case under investigation refers to doubly periodic arrays of straight parallel circular fibre-like inclusions embedded into a surrounding matrix, both made of homogeneous isotropic linear elastic material. Theoretically, the above mentioned problem is posed on the so called *unit cell* domain as a secord order elliptic problem with possibly highly oscillating coefficients and periodicy Dirichlet buoundary conditions for the *cell function* χ [6].

For such a composite, *homogenized* or *equivalent* in-plane shear moduli can be deduced resorting to a closed form solution method proposed in [6], which will serve as a reference for accuracy ascertainment purposes. A numerical tool in this regard is nonetheless of the uttermost importance, because it can deal with material/geometric arrangements and setups for which closed-form solutions of the homogenization problem are not available. Given the particular domain under consideration, the choice of a curved edge VEM approach seems naturally appropriate, aiming at calibration and accuracy assessment of the methodology, and granting a broader range of applicability than periodically arranged purely linear elastic constituents [1].

Without addressing explicitly the numerical approximation of the homogenization problem at hand (the interested reader may find detailed treatment in [3, 1]), we will consider a representative material setup with fibre-to-matrix shear moduli ratio of 50 and perfect interfaces [6]. The discrete domain consists

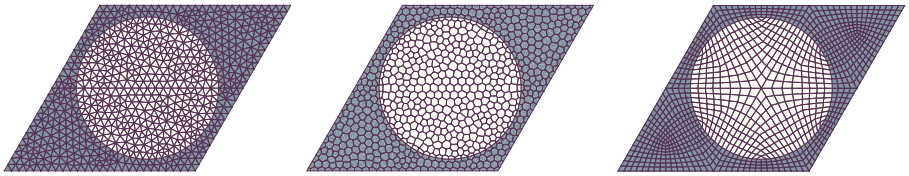

(a) (b) (c)

Figure 7: Asymptotic homogenization. Parallelogram unit cell with circular inclusion ($v_f = 0.5$.) Representative mesh types. (a) Tri-mesh. (b) Voro-mesh. (c) Quad-mesh

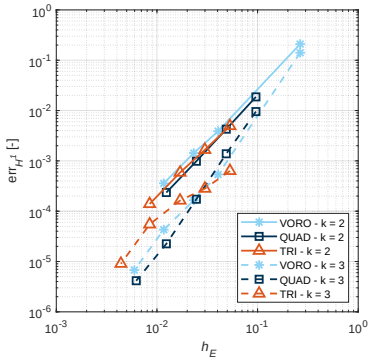

Figure 8: Asymptotic homogenization. H^1 error norm *vs* mesh size h_E for $k = 2$ and $k = 3$ VEM approximations of the homogenization problem.

of a simple polygonal mesh of the unit cell which in the present case is a parallelogram with equal unit sides incorporating a centered circular inclusion as can be seen in fig. 7, where three types of meshes are pictured, namely triangles, quadrilaterals and Voronoi polygons. Quadratic and cubic VEM approximation spaces are here adopted for each mesh, and h-convergence is assessed in terms of H^1 relative error norm for the cell function with respect to the analytical one. As in the previous case, polygons adjacent to fibre-matrix interface have a circular edge, hence they are processed using the presented cubature scheme. As it can be deduced from Fig. 8, all the tested schemes behaves as predicted in terms of convergence rates, with a slight edge in favor of square mesh discretizations for what concerns accuracy.

4 Conclusion

We have constructed low-cardinality algebraic cubature formulas for convex or concave polygonal elements with a circular edge, arising by element intersection or difference with a disk. These situations are typical of computational mechanics models, where convex elements have to be interfaced with a circular inclusion or a circular hole, as discussed above.

It should be stressed that the cubature formulas can be extended to the more general case of elliptical inclusions or holes, that are of great interest in computational mechanics where using classical FEM approaches necessarily implies a rectification error [46, 32] which can significantly affect solution accuracy, whereas it is proved that curvilinear VEM, avoiding such inconvenience, grant superior accuracy at a lower computational cost [7].

Indeed, by an invertible affine transformation (more precisely a roto-translation followed by axes scaling) an ellipse is mapped onto a disk and convex polygonal elements onto elements which remain convex and polygonal. Then we can use the cubature machinery for the circular case and get a formula for the elliptical case by the corresponding change of variables (a Matlab package including the elliptical case is in preparation [8]).

Following current trends in VEM implementations, it is also of great interest the possibility of using general elements with more than one or even all curved edges, not necessarily circular (or elliptical). These cases have been cleverly treated in the recent VEM literature, renouncing however to polynomial exactness, cf. [13]. The construction of algebraic cubature formulas on such elements is another of our future goals, as an application of a general approach to low-cardinality algebraic cubature on Jordan domains with a piecewise regular boundary, approximated to high precision by spline curves (spline curvilinear polygons, [40]).

References

[1] A. Albori, E. Artioli, L. Beirão da Veiga, C. Lovadina, M. Verani, *Curvilinear polygonal virtual elements for asymptotic homogenization problems*, Book of abstracts of the XXII Convegno GIMC, Ferrara (Italy), 13-14 September, 2018.

[2] P.F. Antonietti, P. Houston and G. Pennesi, *Fast Numerical Integration on Polytopic Meshes with Applications to Discontinuous Galerkin Finite Element Methods*, J. Sci. Comput. 77 (2018), 1339–1370.

[3] E. Artioli, *Asymptotic homogenization of fibre-reinforced composites: a virtual element method approach*, Meccanica 53 (2018), 1187–1201.

[4] E. Artioli, L. Beirão da Veiga, C. Lovadina and E. Sacco, *Arbitrary order 2D virtual elements for polygonal meshes: Part I, elastic problem*, Computational Mechanics 60 (2017), 355–377.

[5] E. Artioli, L. Beirão da Veiga, C. Lovadina and E. Sacco, *Arbitrary order 2D virtual elements for polygonal meshes: Part II, inelastic problem*, Computational Mechanics 60 (2017), 643–657.

[6] E. Artioli, P. Bisegna and F. Maceri, *Effective longitudinal shear moduli of periodic fibre-reinforced composites with radially-graded fibres*, Int. J. Solids Struct. 47 (2010), 383–397.

[7] E. Artioli, F. Dassi and L. Beirão da Veiga, *Curvilinear Virtual Elements for 2D solid mechanics applications*, Comp. Meth. Appl. Mech. Eng. (2019), *in press.*

[8] E. Artioli, A. Sommariva and M. Vianello, *ELLPEM: Matlab codes for low-cardinality algebraic cubature on polygonal elements with an elliptical edge*, in preparation.

[9] E. Artioli and R.L. Taylor, *VEM for inelastic solids*, Computational Methods in Applied Sciences 46 (2018), 381–394.

[10] B. Bauman, A. Sommariva and M. Vianello, *Compressed cubature over polygons with applications to optical design*, submitted (2019), `https://www.math.unipd.it/~marcov/pdf/polygons.pdf`

[11] L. Beirão da Veiga, F. Brezzi and L.D. Marini, *Virtual elements for linear elasticity problems*, SIAM J. Numer. Anal. 51(2) (2013), 794–812.

[12] L. Beirão da Veiga, C. Lovadina and D. Mora, *A virtual element method for elastic and inelastic problems on polytope meshes*, Computer Methods in Applied Mechanics and Engineering 295 (2015), pp.327–346.

[13] L. Beirão da Veiga, A. Russo and G. Vacca, *The Virtual Element Method with curved edges*, ESAIM: Mathematical Modelling and Numerical Analysis 53(2) (2019), 375–404.

[14] L. Beirão da Veiga, F. Brezzi, A. Cangiani, G. Manzini, L.D. Marini and A. Russo, *Basic principles of virtual element methods*, Math. Models Methods Appl. Sci. 23(1) (2013), 199–214.

[15] L. Beirão da Veiga, F. Brezzi, L. D. Marini, and A. Russo, *The Hitchhiker's Guide to the Virtual Element Method*, Math. Models Methods Appl. Sci. 24(8) (2014), 1541–1573.

[16] A. Bensoussan, J.L. Lions and G. Papanicolau, *Asymptotic Analysis for Periodic Structures*, North-Holland, Amsterdam, 1978.

[17] F. Brezzi and L.D. Marini, *Virtual element methods for plate bending problems*, Comput. Methods Appl. Mech. Engrg. 253 (2013), 455–462.

[18] C. Caratheodory, *Über den Variabilittsbereich der Koeffizienten von Potenzreihen, die gegebene Werte nicht annehmen*, Math. Ann. 64 (1907), 95–115.

[19] R. Cools, Constructing cubature formulae: the science behind the art, Acta Numer. 6 (1997), 1–54.

[20] R. Cools, An encyclopaedia of cubature formulas, J. Complexity 19 (2003), 445–453.

[21] G. Da Fies, A. Sommariva and M. Vianello, *Algebraic cubature by linear blending of elliptical arcs*, Appl. Numer. Math. 74 (2013), 49–61.

[22] G. Da Fies and M. Vianello, *Trigonometric Gaussian quadrature on subintervals of the period*, Electron. Trans. Numer. Anal. 39 (2012), 102–112.

[23] G. Dasgupta, *Integration within Polygonal Finite Elements*, J. Aerosp. Eng. 16(2003), pp. 9–18.

[24] S. Foucart and H. Rauhut, *A Mathematical Introduction to Compressive Sensing*, Birkhäuser, 2013.

[25] A.L. Gain, C. Talischi and G.H. Paulino, *On the virtual element method for three-dimensional linear elasticity problems on arbitrary polyhedral meshes*, Comput. Methods Appl. Mech. Engrg. 282 (2014), 132–160.

[26] M. Gentile, A. Sommariva and M. Vianello, *Polynomial interpolation and cubature over polygons*, J. Comput. Appl. Math. 235 (2011), 5232–5239.

[27] C.L. Lawson and R.J. Hanson, *Solving least squares problems*, Classics in Applied Mathematics 15, SIAM, Philadelphia, 1995.

[28] S.E. Mousavi and N. Sukumar, *Numerical integration of polynomials and discontinuous functions on irregular convex polygons and polyhedrons*, Comput. Mech. 47 (2011), 535–554.

[29] S.E. Mousavi, H. Xiao and N. Sukumar, *Generalized Gaussian quadraturerules on arbitrary polygons*, Internat. J. Numer. Methods Engrg. 82 (2010), 99–113.

[30] S. Natarajan, S. Bordas and D.R. Mahapatra, *Numerical integration over arbitrary polygonal domains based on Schwarz-Christoffel conformal mapping*, Internat. J. Numer. Methods Engrg. 80 (2009), 103–134.

[31] F. Piazzon, A. Sommariva and M. Vianello, *Caratheodory-Tchakaloff Subsampling*, Dolomites Res. Notes Approx. DRNA 10 (2017), 5–14.

[32] D. Pivovarov, R. Zabihyan, J. Mergheim, K. Willner and P. Steinmann, *On periodic boundary conditions and ergodicity in computational homogenization of heterogeneous materials with random microstructure*, Comp. Meth. Appl. Mech. Eng. 357 (2019), 112563.

[33] M. Putinar, *A note on Tchakaloff's theorem*, Proc. Amer. Math. Soc. 125 (1997), 2409–2414.

[34] E. Sanchez-Palencia, *Non-Homogeneous Media and Vibration Theory*, Lecture notes in physics, Springer, Berlin, 1980.

[35] M. Slawski, *Non-negative least squares: comparison of algorithms*, `https://sites.google.com/site/slawskimartin/code`

[36] A. Sommariva, *Cubature codes and pointsets*, `http://www.math.unipd.it/~alvise/software.html`

[37] A. Sommariva and M. Vianello, *Product Gauss cubature over polygons based on Green's integration formula*, BIT Numerical Mathematics 47 (2007), 441–453.

[38] A. Sommariva and M. Vianello, *Gauss-Green cubature and moment computation over arbitrary geometries*, J. Comput. App. Math. 231 (2009), 886–896.

[39] A. Sommariva and M. Vianello, *Compression of multivariate discrete measures and applications*, Numer. Funct. Anal. Optim. 36 (2015), 1198–1223.

[40] A. Sommariva and M. Vianello, *Tchakaloff-like cubature rules on spline curvilinear polygons*, in preparation.

[41] Y. Sudhakar and W.A. Wall, *Quadrature schemes for arbitrary convex/concave volumes and integration of weak form in enriched partition of unity methods*, Comput. Methods Appl. Mech. Engrg. 258 (2013), 39–54.

[42] Y. Sudhakar, A. Sommariva, M. Vianello and W.A. Wall, *On the use of compressed polyhedral quadrature formulas in embedded interface methods*, SIAM J. Sci. Comput. 39 (2017), B571–B587.

[43] N. Sukumar, D.L. Chopp, N. Moes and T. Belytschko, *Modeling holes and inclusions by level sets in the extended finite-element method*, Computer Methods in Applied Mechanics and Engineering **190** (2001), 6183–6200.

[44] M. Tchernychova, *Caratheodory cubature measures*, Ph.D. dissertation in Mathematics (supervisor: T. Lyons), University of Oxford, 2015.

[45] M. Vianello, *SUBP: Matlab package for subperiodic trigonometric quadrature and multivariate applications*, `http://www.math.unipd.it/~marcov/subp.html`

[46] G. Wang, W. Li, Z. Feng and J. Ni, *A unified approach for predicting the free vibration of an elastically restrained plate with arbitrary holes*, Int. J. Mech. Sci. 159 (2019), 267–277.